

# Processing and characterization of biodegradable polymer nanocomposites: detection of dispersion state

Natalia V. Pogodina · Claire Cerclé · Luc Avérous ·  
Ralph Thomann · Michel Bouquey · René Muller

Received: 28 June 2007 / Accepted: 6 November 2007  
© Springer-Verlag 2007

**Abstract** Nanobiocomposites of poly(lactic acid) (PLA) with 3–5 wt% organically modified montmorillonite (OMMT) were prepared by melt compounding in two different mixers, miniature twin-screw extruder and internal batch mixer, leading to different degrees of dispersion. The progress of dispersion was characterized by melt rheology coupled with light attenuation. Processed PLA/OMMT samples showed percolating networks in the melt, detected by a step increase in low-frequency elastic moduli. The melt elasticity of nanocomposites increased, while the light attenuation coefficient and the loss tangent decreased progressively with mixing energy and reached saturation that can be attributed to the maximum level of clay

dispersion achieved in the present experimental conditions. Results showed that a combination of low-frequency loss tangent and light attenuation coefficient provides a potentially sensitive method for the characterization of the degree of clay dispersion. The direct correlation between light attenuation coefficient and loss tangent follows linear dependence and may open an approach for the rapid inline analysis of the degree of dispersion in melt-processed nanocomposites.

**Keywords** Nanobiocomposites · Degree of dispersion · Percolating network · Light attenuation · Melt elasticity

Paper presented at the 4th Annual European Rheology Conference (AERC), April 12–14, 2007, Naples, Italy.

N. V. Pogodina · C. Cerclé · L. Avérous · M. Bouquey · R. Muller (✉)  
Laboratory of High Technology Polymeric Materials,  
ECPM-LIPHT (UMR CNRS 7165),  
Louis Pasteur University,  
25 rue Becquerel,  
67087 Strasbourg, Cedex 2, France  
e-mail: Rene.Muller@ecpm.u-strasbg.fr

N. V. Pogodina  
e-mail: Natalia.pogodina@ecpm.u-strasbg.fr

C. Cerclé  
e-mail: cerclec@hotmail.fr

L. Avérous  
e-mail: averousl@ecpm.u-strasbg.fr

M. Bouquey  
e-mail: bouqueym@ecpm.u-strasbg.fr

R. Thomann  
Freiburger Materialforschungszentrum,  
Stefan-Meier-Str. 21,  
79104 Freiburg i. Br., Germany  
e-mail: ralf.thomann@mfz.uni-freiburg.de

## Introduction

Polymer–clay nanocomposites (PNC) are multiphase systems based on components with vastly different properties in the nanometer scale. These materials exhibit many unique properties, such as improved thermal stability, reduced flammability, and improved mechanical and barrier properties, which makes them commercially valuable. The uniform and high level of dispersion of nanoscopically sized fillers (exfoliation process) is the key to the valuable properties of PNC. This uniform dispersion of nanofillers on the order of a few nanometers produces large interfacial area. When polymer–nanoparticle interphase is tailored by a certain compatibility level between the phases, nanocomposites show optimized performance.

Several approaches are developed to exfoliate the initially microscopically heterogeneous system to a nanoscopically homogeneous, including solution processing, in situ polymerization, and melt processing technique. The latter one is very attractive for industrial application due to its simplicity. Despite extensive research and vast amount of publications in the field of polymer nanocomposites (Pinnovaia and Beall

2001; Utracki 2004), the industrial fabrication of PNC is still based on a semiempirical approach. The lack of fundamental understanding of interphase–morphology–property relationships in PNC materials limits our possibility to control their processing and performance. The situation is even more complex when PNC are based on environmentally friendly biodegradable polymers. Among those, poly(lactic acid) (PLA) is at present one of the most promising, commercially available biodegradable polymer with a large range of grades (Ray and Okamoto 2003).

The dispersion morphology and the interphase that impart the valuable properties to the PNC material are born at the processing step. Which processing factor imparts the better level of dispersion is still under discussion. High stresses developed in high viscous matrix (Fornes et al. 2001) and long residence times (Dennis et al. 2001) were pointed out as the key parameters for dispersing clay stacks. Recently, it has been shown that better dispersion was achieved in low viscous matrices (Tanoue et al. 2004). Simultaneous rheo-X-ray studies showed (Bousmina 2006) that the best level of the dispersion requires a balance between the diffusion of polymer chains in interlayer spacing and mechanical shearing to break up clay stacks. According to the author, the medium matrix viscosity and two-step processing (low shear followed by high shear) gives optimum results.

Another important question is how to control the degree of clay dispersion. The morphology of the processed nanocomposite is very complex and may include micro-particles, tactoids, and individual layers (Szazdi et al. 2006). Existing experimental methods probe the complex structure of nanocomposites on different length scales. Transmission electron microscopy (TEM) and X-ray scattering provide local structural characterization on a small scale (Fornes et al. 2001; Dennis et al. 2001; Szazdi et al. 2006; Bousmina 2006). Rheological and mechanical tests probe the bulk of the nanocomposite material and sense the changes in the dispersion process of clay agglomerates on a large scale (Wagener and Reisinger 2003; Meincke et al. 2004; Kadar et al. 2006).

The aim of this paper is to study the influence of processing (the type of compounding device, shear rate, mixing time, mixing energy) on the degree of dispersion of clay stacks in a biodegradable polymer matrix with respect to the rheological, structural, and optical properties and to develop an approach for the rapid analysis of the progress of dispersion.

## Experimental part

### Materials

The PLA used in this work was supplied by Nature Work® (Cargill-Dow LLC, USA). As it was reported by Martin and

Avérous (2001), this biodegradable polyester consists of 92% L-lactide and 8% mesolactide contents. The weight-average molecular weight  $M_w=108,000$  g/mol and the polydispersity index  $M_w/M_n=1.7$  were determined by size exclusion chromatography (SEC). The glass transition and melting temperatures as determined by differential scanning calorimetry (DSC) are 60 and 155 °C, respectively. Density is 1.25 g/cm<sup>3</sup> at 25 °C. The organically modified montmorillonite (OMMT) used in this study was supplied by Southern Clay Products (Cloisite® 30B). Cloisite 30B is organically modified by methyl bis-2-hydroxyethyl hydrogenated tallow ammonium. The content in organics is 30 wt% for Cloisite 30B.

### Compounding and specimen preparation

PLA (pellets form) and clay (powder form) were dried overnight at 80 °C under vacuum. Before processing, 3 and 5 wt% of OMMT have been added into the PLA and premixed in a plastic bag. The compounding of PLA/OMMT nanobiocomposites was carried out at 170 °C in the two mixers: Minilab microcompounder (Rheomex CTW5, Thermolectron) and an internal batch mixer (Rheocord 9000, Haake) at different processing conditions, varying screw speed, and mixing time. The Minilab is a miniature twin-screw extruder with a small filling polymer mass of 5–6 g and an automatic bypass for recirculation. The microcompounder can be equipped with conical corotating or counterrotating screws. The Rheocord 9000, Haake internal batch mixer operates with two blades in counterrotating configuration and a much bigger polymer mass, about 50 g.

### Rheological characterization

The samples processed in both mixers were compression molded into 25 mm diameter disks, 1 mm thick, at 170 °C between two metal blocks lined with Teflon-coated foil using a heated laminating press.

These disks were used for rheological experiments. Dynamic rheological measurements were performed using an advanced rheometric expansion system (ARES) from Rheometrics (TA Instruments). The measurements were carried out in an oscillatory mode using parallel plates (25 mm diameter) at 170 °C. Frequency sweeps were carried out in the range 0.01–100 rad/s at the strain amplitude of 10% to stay in linear viscoelastic range.

### Light attenuation

Turbidity was measured at room temperature on solid samples, compression molded as discussed above into disks, 1 mm thick and 25 mm diameter. Linearly polarized light from a 1-MW He–Ne laser (wavelength 632.8 nm)

passes through the sample and is focused by an objective on a silicone photodiode (Thorlabs, DET 36A/M) for intensity recording, using a data acquisition board (National Instruments, NI-USB-6009). The transmitted intensity from pure laser and from all the samples was monitored with a sampling rate of 0.2 s for 5 min at three different positions for each sample. The results were averaged to minimize the error from possible intensity fluctuations caused by the laser. The averaged intensities have been used to estimate the attenuation coefficient.

### X-ray diffraction

The small angle X-ray scattering (SAXS) measurements were carried out on a powder diffractometer Siemens D 5000 (Germany) using Cu ( $K\alpha$ ) radiation,  $\lambda=0.15406$  nm, in the range of  $2\theta=1.0^\circ$  to  $10^\circ$  by step of  $0.05^\circ$  per 1 s. SAXS analysis was performed at room temperature for pure Cloisite 30B and nanocomposite samples, processed in the batch mixer and in the microextruder. For these tests, the specimens were prepared by compression molding at  $T=170$  °C, as already described above.

### Mechanical characterization

After melt processing, the molten materials were injection molded (170 °C, 250 MPa) in the shape of standard dumbbell specimens (tensile bar ASTM D638), using the minijet injection molding machine (Thermo Electron Corporation, Germany).

Tensile tests were performed for PLA and all samples with a MTS 2/M instrument (Adamel Lhomargy, Ivry sur Seine, France) at room temperature with a speed of 5 mm/min.

## Results and discussion

### Mixing

Compounding of the nanocomposites was performed with intensive mixing in the internal batch mixer and in the miniature twin-screw extruder with corotating configuration of screws where the clay stacks and polymer matrix are subjected to shearing in the flow field.

Both rotational mixers have been approximated by the Couette geometry. The shear rate is then given by (Maric and Macosko 2001):

$$\dot{\gamma} = \frac{D\Omega}{2h} \quad (1)$$

where  $D$  is the average screw diameter,  $h$  is the average gap between the screws and the barrel,  $\Omega=2\pi N/60$  is the angular velocity in rad/s, and  $N$  is the screw speed in

revolution per minute. Index 1 is used for the Minilab and index 2 is used for the internal batch mixer. Equation 1 gives only a rough approximation of the “average” shear rate. As it has been shown by Bousmina et al. (1999), local shear rates can be orders of magnitudes different at various locations, especially if two different mixers with different screw configurations and different flow fields are compared.

The Minilab has conical screws, so the average  $D_1$  and  $h_1$  values have been taken in the middle of the screw  $D_1=10$  mm,  $h_1=0.5$  mm. For the Haake batch mixer:  $D_2=36$  mm,  $h_2=2$  mm. The screw speeds for the batch mixer were  $N_2=50$  and 100 rpm. For the Minilab, a broader range of mixing speeds (and shear rates) was explored:  $N_1=12$ , 25, 50, 100, and 200 rpm. The maximum average shear rate achieved in the batch mixer was  $600^\circ \text{ s}^{-1}$ , while in the Minilab it was twice as large  $1,314^\circ \text{ s}^{-1}$ . The mixing times in the batch mixer were correspondingly  $t_2=5$ , 10, and 20 min, while in the miniextruder, the longer times have been used:  $t_1=7$ , 15, 30, and 50 min. Thus, higher shear rates and higher total strains have been applied in the Minilab.

Because we used two different mixers with different capacities and varied processing conditions, it was reasonable to compare the resultant characteristics of the processed nanocomposites as a function of mixing energy  $E$ . For the rotational mixer, the mixing energy per unit mass can be expressed as:

$$E = \frac{T\Omega t}{M} \quad (2)$$

where  $T$  is the torque,  $t$  is the mixing time, and  $M$  is the loaded mass. Due to longer mixing times and higher mixing speed, the maximum mixing energy achieved in the Minilab was about four times higher than in the batch mixer.

### Melt rheology

Rheology probes the material properties in the bulk. So it has the advantage of being able to detect the three-dimensional superstructures. Especially fruitful are rheological experiments in the small amplitude oscillatory shear (SAOS) mode. First, SAOS uses small strain amplitudes and consequently does not disrupt the possible network formation. These conditions are especially important for nanocomposites which incorporate stiff anisometric clay particles in the matrix. Second, dynamic moduli in the low-frequency range respond very sensitively to the melt elasticity and to the formation of three-dimensional structures. Network formation has been reported in various nanocomposite systems (Wagener and Reisinger 2003; Meincke et al. 2004; Kadar et al. 2006).

A rheological method for the detection of network-like structure formation was proposed by Winter and Mours

(1997). Although originally the method was developed for the detection of chemical gelation (upon the increasing degree of crosslinking), it was successfully used later for the detection of physical gels during crystallization in semicrystalline polymers and gel-like structures in long-chain branched polymer melts.

According to the authors, at the critical gel point, the low-frequency dynamic moduli show a power law behavior:

$$G_c' = \frac{G_c''}{\tan \delta_c} = S_c \Gamma(1 - n_c) \cos \frac{n_c \pi}{2} \omega^{n_c} \quad \text{for } \omega < 1/\lambda_0 \quad (3)$$

where  $S_c$  and  $n_c$  are the gel stiffness and the relaxation exponent, respectively, and  $\lambda_0$  is the lower crossover. All three parameters depend on the material structure at the transition.  $\Gamma$  is the gamma function. A consequence of this power law behavior (at the gel point) is a frequency-independent loss tangent in the terminal zone.

$$\tan \delta_c = \tan \frac{n_c \pi}{2} = \frac{G''}{G'} = \text{const} \quad (4)$$

The formation of a network-like structure (the instant of the liquid-to-solid transition, i.e., critical gel point) is identified by  $\tan \delta(\omega)$  becoming independent of the frequency in the terminal zone according to Eq. 4. After the gel point, i.e., after the liquid–solid transition, the network also exists and the material shows solid-like behavior, which is identified by the positive slope of  $\tan \delta(\omega)$  in the terminal zone.

Figure 1a and b shows the evolution of the storage modulus and  $\tan \delta$  as a function of frequency  $\omega$  for the pure PLA and PLA–clay systems processed in two different mixers with varying shear rates and mixing time. Within the accessible frequency range,  $G'$  for pure PLA is close to the typical low-frequency asymptote of slope 2 for a viscoelastic liquid. The PLA–clay samples reveal in the terminal zone progressively higher elasticity (higher values of the dynamic moduli  $G'$ ,  $G''$ , and lower phase angle). Melt elasticity increases with the increase of the screw speed (shear rate), mixing time, and clay concentration. The fact that, for a given mixing device, the mixing time is suited for better dispersion indicates the eventual role of diffusion in the dispersing process. Moreover, there is a great difference in the rheological response of PLA–clay systems processed in the two different mixers: the low-frequency storage modulus of nanocomposites processed in the Haake batch mixer is one order of magnitude higher and nearly frequency-independent, while the elastic response of nanocomposites processed in the Minilab microextruder is much weaker for the same concentration 3 wt% (Fig. 1a). We argue that this drastically different level of melt elasticity is due to the different degree of clay dispersion in processed nanocomposites, which results in morphologically different network structures.

Figure 1b shows that in the low-frequency range, the slope of  $\tan \delta(\omega)$  changes from negative for pure PLA (typical for the liquid-like behavior) to positive for PLA–clay (typical for the solid-like behavior). It means that the solid-like network of percolating nanoclay fillers in the PLA matrix is monitored for PLA nanocomposites processed in both mixers.

Another representation of the network formation phenomena is given by the van Gurp plot. In the van Gurp plot, the phase angle  $\delta = \arctan G''/G'$  is plotted vs the complex

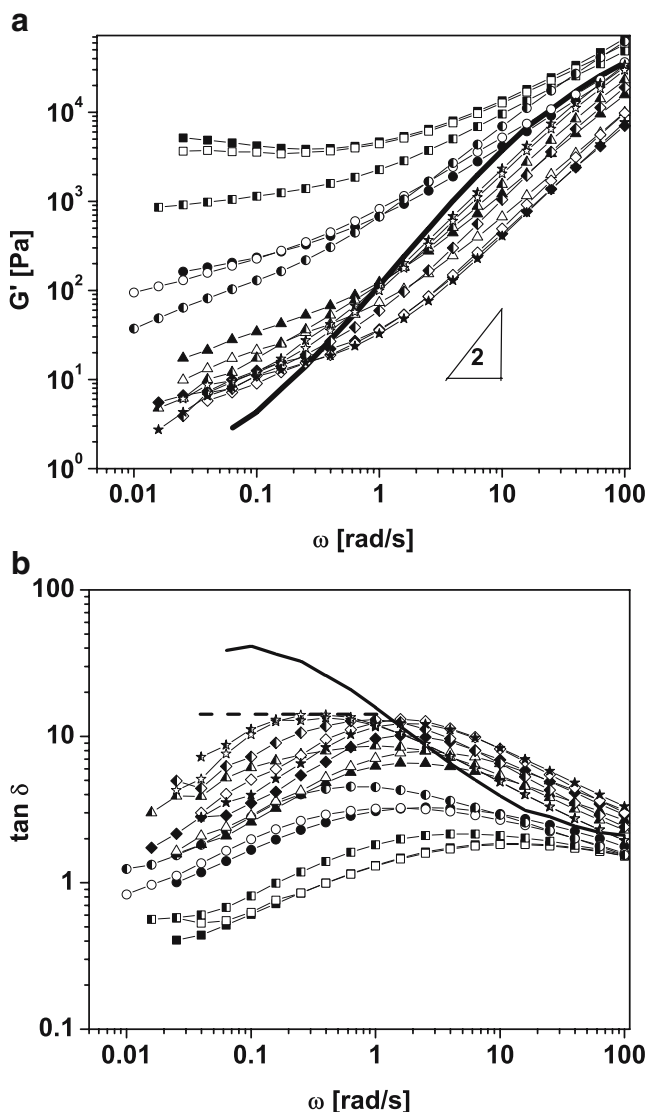


**Fig. 1** Evolution of **a** storage modulus and **b** loss tangent for the PLA, PLA/OMMT-3 wt%, and PLA/OMMT-5 wt% compounded at different processing conditions and in two mixers. The gel point in **b** is marked by a dashed line. Squares PLA-5wt%OMMT batch mixer 100 rpm, circles PLA-3wt%OMMT batch mixer 100 rpm, triangles PLA-3wt% OMMT miniextruder 200 rpm, diamonds PLA-3wt% OMMT miniextruder 100 rpm, stars PLA-3wt%OMMT miniextruder 25 rpm. In each series of symbols, solid symbols correspond to long mixing time, open symbols to intermediate time, and half open symbols to short mixing time; solid line pure PLA;  $T=170$  °C